

# Evaluation of Inherent Damping Introduced by Thyristor Controlled Series Compensators

D. R. WEERAKOON<sup>1</sup> (Graduate Student Member, IEEE),  
C. KARAWITA<sup>2</sup> (Senior Member, IEEE), AND U. D. ANNAKAGE<sup>1</sup> (Senior Member, IEEE)

<sup>1</sup>Department of Electrical and Computer Engineering, University of Manitoba, Winnipeg, MB R3T 2N2, Canada

<sup>2</sup>Transgrid Solutions Inc., Winnipeg, MB R3T 6C2, Canada

CORRESPONDING AUTHOR: D. R. WEERAKOON (diliniibuddhima@gmail.com)

This work was supported in part by the RTDS Technologies Inc., and in part by the Mitacs Accelerate Fellowship.

**ABSTRACT** Series compensation of transmission lines increase the risk of Sub-Synchronous Resonance (SSR) problems. Use of Thyristor Controlled Series Compensators (TCSC) in place of Fixed Series Capacitors (FSC) has benefited in terms of damping SSR. SSR Damping with TCSC can be achieved with supplementary controls or through its inherent damping capability. Use of discrete time models for small signal stability analysis of TCSC is well established. This paper uses a simplified Dynamic Phasor (DP) model of the TCSC for an in-depth evaluation of the inherent SSR damping capability through small signal stability analysis. Source of inherent damping in open loop operation and the representation of it in the DP model is elaborated and the small signal model is validated against Electro Magnetic Transient (EMT) simulations. Effect of inductive-resistive nature of the TCSC on Induction Generator Effect (IGE) and Torsional Interactions (TI) is shown through small signal stability assessment. It is shown that the network resonant frequency exists only in a narrow range of firing angles of the TCSC and thus IGE and TI are avoided in most part of its operating range. IEEE first benchmark system for SSR studies is used to demonstrate the inherent damping capability of a TCSC.

**INDEX TERMS** Dynamic phasors, induction generator effect, inherent damping, sub-synchronous resonance, thyristor controlled series compensator, torsional interactions.

## I. INTRODUCTION

**S**ERIS compensation of transmission lines has long been in use to facilitate long distance ac power transmission. It is known to improve the power transfer capability and enhance the transient stability limits of the power system [1]. However, the presence of Fixed Series Compensators (FSC) in the network may cause adverse interactions with other power system devices such as Conventional Turbine Generators (CTG) and power electronic converters [1], [2]. Sub-Synchronous Resonance (SSR) is a phenomenon which arises when the electrical network interacts with the mechanical and/or electrical system of CTG at frequencies below the nominal frequency of the system [3]. SSR can occur in three types namely: a) Induction Generator Effect (IGE), b) Torsional Interactions (TI), and c) Torque amplification [4]. IGE is purely an electrical phenomena and is caused due to the self excitation of the electrical system. The rotor of a synchronous generator presents a negative resistance at sub-synchronous frequencies when viewed from the stator, thus acting as an induction generator for sub-synchronous currents. IGE

occurs when the positive resistance of the network is less than the negative resistance presented by the generator rotor at sub-synchronous frequencies. This may lead to sustained or growing sub-synchronous oscillations. On the other hand, TI occur when the network resonant frequency is close to any of the torsional modes of the turbine generator shaft system. It can lead to sustained or growing torsional oscillations if the inherent mechanical damping of the torsional system is insufficient. SSR phenomenon has been extensively studied since the first two consecutive incidents which occurred at Mohave generating station in Southern Nevada in 1970 & 71 [5]. The incident has resulted in severe damage to turbine generator shafts where the main cause was identified as the series compensation of transmission lines which lead to TI. Apart from SSR incidents related to CTG, many SSR events related to Type 3 wind power plants are also reported [6], [7]. It is shown in [6] and [7] that the Rotor Side Converter (RSC) controls makes the wind plant vulnerable to SSR conditions and produce a negative resistance at slip frequencies in the presence of series compensation.

Thyristor Controlled Series Compensator (TCSC) is a Flexible AC Transmission System (FACTS) device which allows rapid and continuous control of series compensation level of transmission lines and hence provide flexible power transfer capability. It can be effectively utilized to damp power system oscillations and mitigate SSR [8]. In practical TCSC projects, methods such as damping torque coefficient and frequency scanning are used to analyze the SSR phenomena [9], [10], [11]. However, small signal stability tools give insight into sensitivity of different parameters, participation of states in different modes, and it is useful in optimization of controllers. The best practice would be to first evaluate the risk of SSR using small signal stability techniques and then verify the findings through non-linear time domain simulations (e.g. Electro Magnetic Transient-EMT).

In general, TCSC contributes to solve SSR in two different ways: “inherent damping” and damping introduced using a supplementary controller. The latter technique is mainly evaluated in practical projects. The “inherent damping” is the amount of damping that can be obtained without adding an additional Sub-Synchronous Damping Controller (SSDC). Many studies have been conducted on damping SSR with TCSC via supplementary control schemes such as SSDC [9], [12], [13]. Such techniques modulate the firing angle to introduce damping. In references [10], [11], and [14], a special thyristor control technique called Synchronous Voltage Reversal (SVR) is used to control the TCSC by controlling the zero crossings of the capacitor voltage. However, in this work, the conventional direct control of the firing angles of thyristors is analysed. When the TCSC is operating in capacitive vernier mode without any supplementary controls, its inherent behaviour in the sub-synchronous frequency range is useful in mitigating SSR in some cases as shown by [15] and [16]. However, the mechanism behind the inherent behaviour of the TCSC in terms of avoiding SSR conditions has not been well explained. Due to the growing number of SSR issues in the power electronic dominated power systems, industries have the incentive to make significant investments on TCSCs instead of FSCs. Thus, the main objective of this paper is to show how the inherent behaviour of the TCSC avoids potential SSR conditions, which can be utilized to avoid existing SSR conditions. For the simplicity, the TCSC was mainly analysed in constant firing angle mode. In addition, the effect of closed loop current controller was also evaluated. The contributions of this paper are as follows.

- The mechanism within the TCSC that leads to inherent damping is explained.
- Assessed the adequacy of a simplified Dynamic Phasor (DP) model of the TCSC for small signal stability analysis.
- Applied the validated DP model of the TCSC to analyse the effect of inherent damping nature of the TCSC on IGE and TI.

A review of the past work conducted on inherent damping nature of the TCSC and available TCSC models for SSR studies are briefed in section II.

## II. LITERATURE REVIEW

### A. INHERENT DAMPING OF TCSC

Considerable efforts have been taken and reported in literature to explore the SSR damping capability of the TCSC in open loop operation. Simulator tests on the first TCSC installation at Kayenta substation in 1990 [17] shows that the TCSC impedance in open loop configuration exhibits a resistive-inductive nature for sub-synchronous frequencies, providing positive damping to SSR conditions. A study on the second TCSC installation at BPA’s (Bonneville Power Administration) Slaat substation in 1995 [18] has showed that the TCSC operating in impedance control mode makes the electrical system behave like an uncompensated system in terms of the electrical damping torque observed at the synchronous machine. The frequency response of one of the segments of TCSCs at slaat [15] shows that the electrical resonant condition is avoided through TCSC by changing its capacitive reactance at sub-synchronous frequencies and introducing an equivalent resistance. Work in [19] has shown that the TCSC behaves as a positive resistance in series with a small inductance at sub-synchronous frequencies.

In an effort to identify the source of resistance in the open loop operation of the TCSC at sub-synchronous frequencies, [20] shows that a virtual resistance appears in the TCSC due to the switching action. It has also shown that apart from the positive resistance at sub-synchronous frequencies, TCSC also exhibits a slight negative resistance at the synchronous frequency. This resistive performance at synchronous and sub-synchronous frequencies is explained in terms of the power conversion ability in [21]. It is shown the power loss at the sub-synchronous frequency is apparently injected into the synchronous frequency which appears as a negative resistance. In this work, the source of inherent damping in open loop operation is explained through a simplified DP based small signal model of the TCSC upon validation against EMT simulations. The same model is then used to demonstrate how this inherent damping nature effects SSR in terms of IGE and TI, throughout the operating range of the TCSC. Understanding this is useful in avoiding potential SSR conditions in the power system at the design stage.

### B. TCSC MODELS

TCSC is a non-linear device which involves both continuous and discrete events. The non-linearity can be handled well with EMT models and compared to other simulation models, they are the closest prediction of the performance to the real device. Quasi-steady state models of TCSCs are not suitable for SSR analysis as it omits important dynamics of TCSC such as the inductor current dynamics, in sub-synchronous frequency range. Modelling techniques reported in literature which are suitable for SSR, can generally be categorized as, a) Discrete time modelling, b) DP modelling, and c) Numerical modelling with frequency scanning. Discrete time models of TCSC have been developed based on the theory of Poincare mapping in [22], [23], [24], [25], [26], [27], and [28]. The

small signal stability is assessed based on the eigenvalues of the Jacobian of the Poincare map. Discrete models developed in [22], [23], and [24] lacks modularity, where the rest of the power system has to be also discretized. However, [25] and [26] has converted the discrete time model to a continuous model based on the assumption that the interfacing quantities of the TCSC with the network is constant over a half cycle period. But, as stated by authors of [26], the validity of modelling approach is questionable if the TCSC accounts for a large portion of the total compensation level. However, the inherent damping associated with open loop operation of the TCSC is accurately represented by these discrete models. Previously discussed models are based on two samples per cycle, limiting the bandwidth to 120 Hz. Model derived in [27] has increased the bandwidth by accommodating six samples per cycle. However, the model is sample variant and not modular. The modularity of six samples per cycle model is achieved in [28] by assuming linear variation of interface variables in contrast to assuming them constant as in [25] and [26].

Work presented in [12] uses frequency scanning to numerically obtain small signal frequency response of the system through time domain simulations. Then the frequency response matrix of the TCSC is fitted to a rational transfer function using vector fitting technique which is then converted to state-space form and combined with the state space model of the rest of the system. This method is accurate for analysing the stability but, it lacks information about the physical states and the results depends on the measurement parameters such as filter constants. Furthermore, it may result in unexplainable eigenvalues when trying to fit the frequency response, specially for large power systems.

The concept of time varying Fourier coefficients has been first applied to TCSCs in [29] to obtain a fundamental frequency DP model of the TCSC. DP modelling of TCSC leads to simple yet powerful models, which are modular in nature and computationally efficient. These models are compatible with phasor based representation of other power system components and therefore can easily be implemented in commercial small signal stability assessment tools. A simplified version of the same model has been used to analyse the SSR behaviour in [30]. The large signal dynamic phasor model in [29] has been extended to include the dynamics of higher order harmonic terms of TCSC in [31]. However, the work does not investigate the small signal stability of the model.

This paper will extend the validation and application of the DP model in [31] for small signal stability analysis of SSR. The model in [31] is simplified and validated against responses from electromagnetic simulation program PSCAD/EMTDC™. The simplified model is then used to evaluate the inherent damping of the TCSC using IEEE 1<sup>st</sup> Benchmark for SSR studies. The organization of the paper is as follows. The basic operation of the TCSC and the behaviour of the TCSC during a disturbance is discussed in section III. For reasons of clarity, Section IV describes the

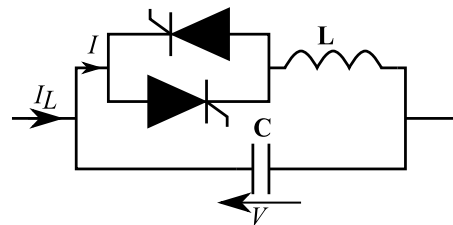


FIGURE 1. Structure of a TCSC.

chosen DP model. It includes the simplification carried out to the model and the method of integration to the network. The representation of the non-linear switching behaviour in the model is highlighted in the same section. Section V compares time domain responses of the small signal model against EMT simulations. It further explains the mechanism within the TCSC that leads to inherent damping in open loop operation. Finally, the effect of the inherent SSR damping capability of the TCSC on IGE and TI are analysed in Section VI, followed by concluding remarks.

### III. TCSC OPERATION

A TCSC is a parallel combination of a fixed capacitor and a Thyristor Controlled Reactor (TCR) as shown in Fig. 1. Thyristors are switched at the supply frequency with a delay angle ' $\alpha$ ', synchronized to the zero crossings of either the line current ( $I_L$ ) or capacitor voltage ( $V$ ). The firing angle ' $\alpha$ ' will eventually control the inductance in TCR branch. In this work, firing angles are synchronized to zero crossings of the line current through a Phase Locked Loop (PLL), which is preferred over the other method due to relatively less harmonic distortions present in the line current. TCSC can behave as an equivalent inductor or a capacitor at the synchronous frequency depending upon the firing angle. It is usually operated in capacitive region or in blocked thyristor mode. Operation near the parallel resonance (point at which the TCSC reactance change from inductive to capacitive or vice versa) should be avoided for stable operation. The firing angle can be maintained fixed or synthesized by upper layer controllers such as current, voltage or power flow controllers which may also include auxiliary controls such as Power Oscillation Damping Controllers (PODC) and SSDC. The inherent damping of the TCSC must be studied in the absence of TCSC supplementary controllers.

Performance of the TCSC in a network is mainly governed by three parameters which can also be considered when sizing a TCSC. They are, a) The level of controllable series compensation ( $X_{TCSC}$ ), b). Boost Factor ( $Kb$ ), and c) Characteristic Factor ( $\lambda$ ) as described by (1), (2), and (3) respectively.

$$X_{FSC} + X_{TCSC} = X_{TOT} \quad (1)$$

$$Kb = \frac{X_{TCSC}}{X_C} \quad (2)$$

$$\lambda = \frac{\omega_N}{\omega_0} = \sqrt{\frac{X_C}{X_L}} \quad (3)$$

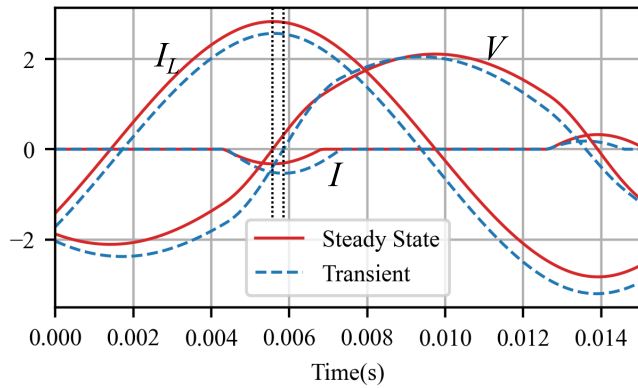


**FIGURE 2. Steady state and transient waveforms of TCSC operating in capacitive region ( $I_L$ : Line current,  $I$ : TCR current and  $V$ : TCSC voltage).**

$X_{FSC}$  is the amount of FSC out of total series compensation level of  $X_{TOT}$  and  $X_C$  &  $X_L$  are the reactance of ‘L’ and ‘C’ respectively at the synchronous frequency. Term  $\omega_N$  in (3) is the resonant frequency of ‘L’ and ‘C’ ( $\sqrt{\frac{1}{LC}}$ ) and  $\omega_0$  is the synchronous frequency. Size of ‘L’ and ‘C’ of the TCSC can be determined using (2) and (3) with proper choice of  $Kb$  and  $\lambda$ . Value of  $Kb$  is typically chosen to be less than 3 to avoid operation near the resonant region [32] and typical values of  $\lambda$  are in the range from 2 to 4 to avoid multiple parallel resonant points. The effect of these parameters on the inherent damping capability of the TCSC will be discussed in Section VI through eigenvalue analysis.

Fig. 2 illustrates the EMT waveforms of a TCSC operating in capacitive vernier mode in steady state and during a disturbance. The behaviour of a TCSC is non-linear because the thyristor turn-off times depend on the TCR current. Transient waveforms are obtained by superimposing a small voltage at sub-synchronous frequency to one end of the transmission line with a TCSC. In steady state, the negative peak of the TCR current, zero crossing of TCSC voltage and the positive peak of the line current are in exact coincidence. During a disturbance, thyristors are fired at the same instant as in steady state, but the conduction time is longer. Thus, the negative peak of the TCR current and the zero crossing of the TCSC voltage do not coincide with the positive peak of the line current. There is a phase shift between the positive peak of the line current and the negative peak of the TCR current (so does the zero crossing of the capacitor voltage). This phenomenon can be thought of as a dynamic resistance which appears in series with the TCSC only during a disturbance adding damping to the circuit. The dynamic resistance which appears due to the non-linearity in switching behaviour contributes to the inherent damping capability of the TCSC as will be shown in Section V.

#### IV. DYNAMIC PHASOR MODELLING OF TCSC

Natural state variables of the TCSC can be chosen as capacitor voltage ‘v’ and TCR current ‘i’ and their behaviour can be characterized by two differential equations (4) & (5), where

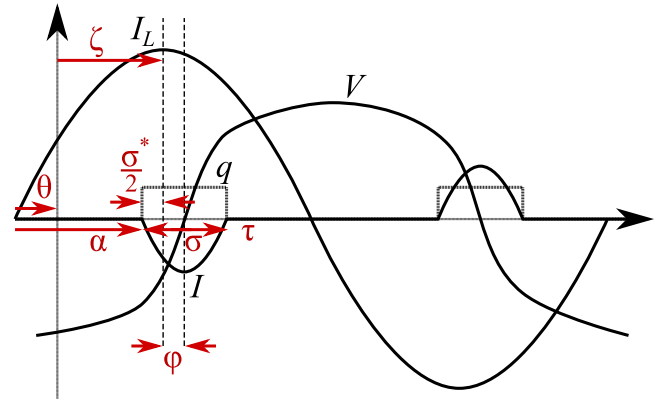


**FIGURE 3. Waveforms of the TCSC during a disturbance, when operating in capacitive region.**

‘ $q(t)$ ’ denotes the switching function and ‘ $i_L$ ’ is the line current.

$$C \frac{dv(t)}{dt} = i_{L(t)} - i(t) \quad (4)$$

$$L \frac{di(t)}{dt} = q(t)v(t) \quad (5)$$

The dynamic phasor model of (4) & (5) is obtained with first principles of time varying Fourier co-efficients in [29]. The 3<sup>rd</sup> and 5<sup>th</sup> harmonic content in the TCSC voltage is significant when the thyristor conduction angle is high. Therefore, the model can be extended to include the dynamics of 3<sup>rd</sup> and 5<sup>th</sup> harmonic phasors of the TCSC voltage and TCR current as explained in [31]. Finally, the DP model is obtained as in (6) & (7) with  $k = 1, 3$  & 5 (Subscript ‘k’ denotes the harmonic number.).

$$C \frac{dV_k}{dt} = I_{L_k} - I_k - jC\omega V_k \quad (6)$$

$$L \frac{dI_k}{dt} = \langle qv \rangle_k - jL\omega I_k \quad (7)$$

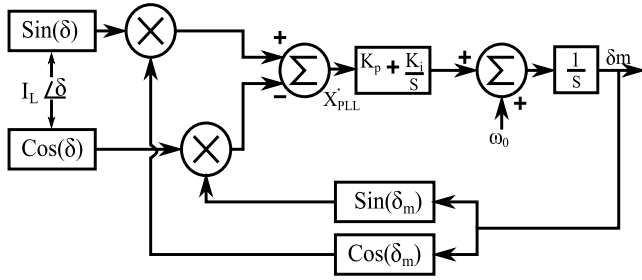
The term ‘ $\langle qv \rangle_k$ ’ in (7) is a non-linear term and can be expanded with the property of convolution in phasor domain according to (8) and since ‘q’ and ‘v’ are real quantities, the relationship in (9) is valid.

$$\langle qv \rangle_k = \sum_{i=-5, -3, -1, 1, 3, 5} \langle q \rangle_{k-i} \langle v \rangle_k \quad (8)$$

$$\langle v \rangle_{-k} = \langle v \rangle_k, \langle q \rangle_{-k} = \langle q \rangle_k \quad (9)$$

Thereafter, the accuracy of the model depends on how well the non-linearity in the switching term ‘ $\langle q \rangle_k$ ’ is estimated. To arrive at an expression for ‘ $\langle q \rangle_k$ ’, consider the representation of TCSC waveforms during a disturbance as in Fig. 3. The non-linearity in switching is represented as a phase shift ‘ $\phi$ ’ between the opposite polarities of the line current and TCR current which accounts for the dynamic resistance. Phase shift ‘ $\phi$ ’ only exist during disturbance and is zero at steady state. Term ‘ $\langle q \rangle_k$ ’ is the average of the switching function ‘q’ for half a cycle period and it depends on the turn-on and turn-off instants of thyristors. The turn-on




**FIGURE 4. Block diagram of the PLL.**

instant depends on the controller and/or the synchronization scheme and therefore can be expressed as, ' $\zeta - \frac{\sigma^*}{2}$ ', where ' $\zeta$ ' (phase angle of the peak of the line current) is from the PLL and ' $\sigma^*$ ' is generated from controllers. The turn-off instant can be expressed as ' $\zeta + 2\phi + \frac{\sigma^*}{2}$ ' and it depends further on the zero crossing of TCR current which is included in angle ' $\phi$ ' as in (13). Taking these instants into consideration, an expression for ' $\langle q \rangle_k$ ' is arrived as in (10) & (11) [31].

$$\langle q \rangle_k = \frac{2}{k\pi} \sin\left(\frac{k\sigma}{2}\right) e^{-jk(\zeta + \phi)} \quad (10)$$

$$\langle q \rangle_0 = \frac{\sigma}{\pi} \quad (11)$$

where,

$$\sigma = 2\left(\frac{\pi}{2} + \phi - \alpha\right) \quad (12)$$

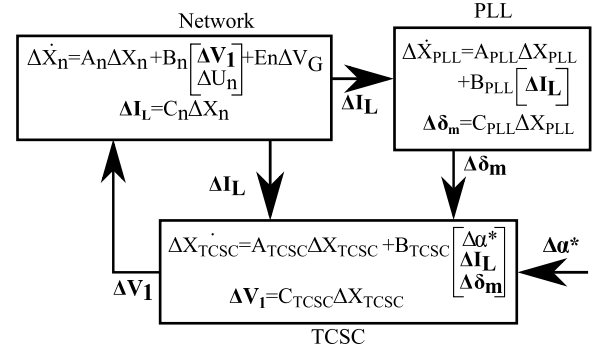
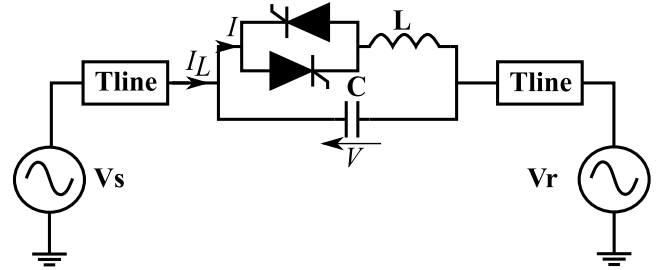
$$\phi = \angle -I_1^* I_{L1} \quad (13)$$

As transmission lines are highly inductive, the line currents are assumed to be essentially sinusoidal (free from harmonic distortions) and it is a valid assumption based on the time domain simulations. Therefore,  $I_{L3,5} = 0$ . The sixth order complex state space model in (6) & (7) is separated into real and imaginary components and linearized around a certain operating point to form a 12<sup>th</sup> order model. However, it was noted that the dynamics of 3<sup>rd</sup> and 5<sup>th</sup> harmonics of the TCSC voltage and TCR current corresponds to very fast dynamics and the linearization makes the small signal model unstable at certain operating points. Therefore, the dynamics of higher order terms were ignored after linearization as in (14) & (15) and the relevant variables ( $V_3, V_5, I_3$  &  $I_5$ ) were treated as algebraic quantities. The simplified model can be combined with the rest of the network which is primarily fundamental frequency based. This simplification will reduce the size of the state matrix to the order of 4, reducing the computational burden when it comes to handling large networks while retaining important dynamics of the TCSC for SSR analysis.

$$\frac{d\Delta V_{i=3,5}}{dt} = 0 \quad (14)$$

$$\frac{d\Delta I_{i=3,5}}{dt} = 0 \quad (15)$$

The synchronization scheme plays an important role in TCSC dynamics. A simplified version of the PLL is used based on the assumption that the three phases are balanced and is shown in Fig. 4 [33]. The PLL model introduces two


**FIGURE 5. Combination of the small signal models of TCSC, PLL and network.**

**FIGURE 6. Test system with a series compensated line.**
**TABLE 1. Test system parameters.**

Parameter	Value	Parameter	Value
$V_s$	$1 \angle 0$ pu	$V_r$	$1 \angle -15^0$ pu
$X_L$	0.0136 pu	$X_C$	0.0603 pu
PLL $K_p$	50 rad/s	PLL $K_i$	900 rad/s <sup>2</sup>
T-line	$0.2808 \angle 86.5^0$ pu		

Impedances and voltages are expressed in the base of 1000 MVA and 500 kV respectively at 60 Hz nominal frequency

new state variables ' $X_{PLL}$ ' and ' $\delta_m$ '. The actual phase angle ' $\delta$ ' is the angle of phasor ' $I_{L1}$ '. The TCSC model along with the PLL is included in the linearized network equations to obtain the small signal model of the entire network as shown in Fig. 5. It should be noted that the power frequency admittance matrix representation of the network is not adequate for SSR analysis as it ignores network dynamics. Thus, a DP representation of the network [33] is used in this work (Dynamics of inductor current and capacitor voltage phasors are considered). Furthermore, to be consistent with the representation of the network and the TCSC, any conventional generators in the network must be modelled considering their stator dynamics as in [33]. As seen from Fig. 5, inputs to the TCSC are the network current ' $I_L$ ', PLL angle ' $\delta_m$ ', and the firing angle order ' $\alpha^*$ ' (which is generated from upper layer controls) and the output to the network is the TCSC fundamental voltage phasor ' $V_1$ '. Matrices  $A$ ,  $B$ , and  $C$  are the state, input and output matrices of respective elements. Note the term ' $V_G$ ' are the bus voltage matrix at generator interfacing buses if there are any.

## V. TCSC MODEL VALIDATION

In order to validate the simplified DP small signal model of the TCSC, a test circuit is formed with a series compensated

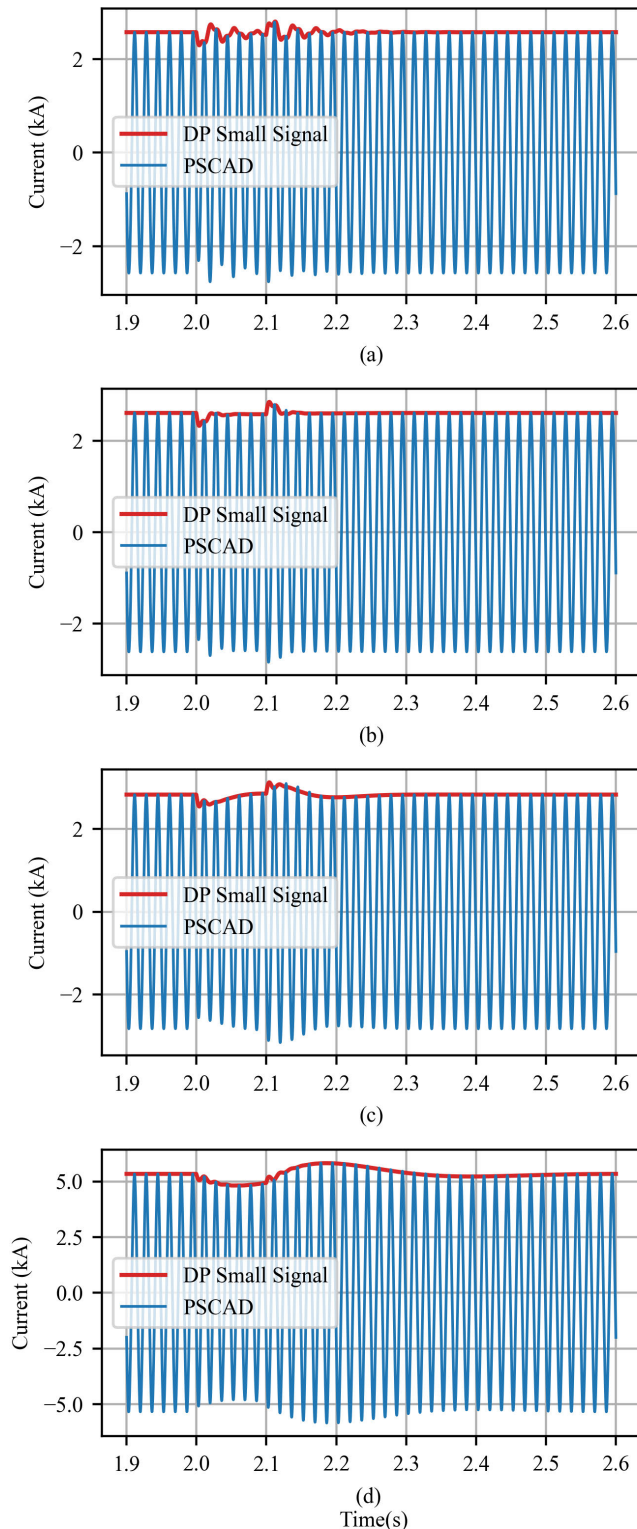


FIGURE 7. Comparison of line current responses for firing angles (a)  $\alpha = 83^\circ$ , (b)  $\alpha = 73^\circ$ , (c)  $\alpha = 63^\circ$ , & (d)  $\alpha = 53^\circ$ .

transmission line connecting two voltage sources as shown in Fig. 6. Series compensation is fully provided by the TCSC (i.e. no FSC) and is operated with fixed firing angle control. System parameters are given in Table 1.

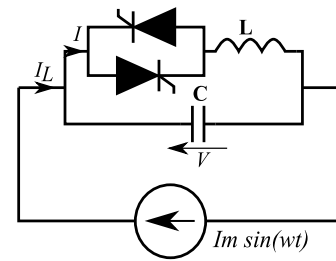


FIGURE 8. TCSC supplied with a constant current source.

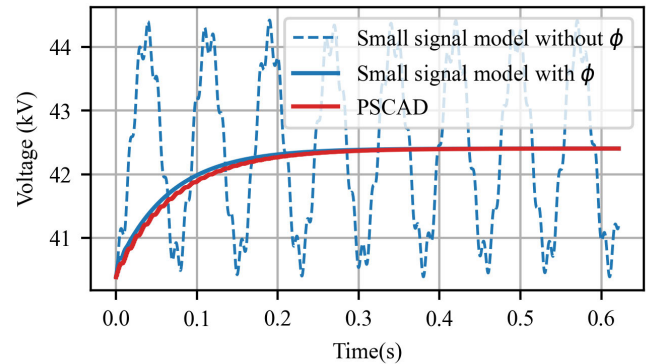


FIGURE 9. Effect of modelling phase shift ' $\phi$ '.

To validate the TCSC model against EMT simulations, a small disturbance of 5% increment to the receiving end voltage ( $V_r$ ) was applied for 100ms at 2s. The model is validated at four different operating points ( $\alpha = 83^\circ, 73^\circ, 63^\circ$ , and  $53^\circ$ ) in the capacitive region. The goal was to validate the model as close as possible to the resonant condition which occurs at  $\alpha = 47^\circ$ . Fig. 7 shows the comparison of line current responses of the small signal model with PSCAD simulations at four operating points. It is observed that the simplified DP small signal model tracks the envelop of the PSCAD waveforms quite accurately.

If we think of the TCSC as a parallel combination of a fixed capacitor and a variable reactor, at steady state in open loop configuration, there should be no damping offered by the parallel  $L-C$  combination to any oscillation. In fact, it should be a marginally stable system, and an oscillatory behaviour is expected. With relevance to that, the following test is conducted to identify the effect of modelling the phase shift ' $\phi$ ' in the DP model of the TCSC. Consider the same TCSC in the previous test system supplied with a constant current source as in Fig. 8. A small disturbance of 5% increment to the input current was applied and the fundamental component of TCSC voltage from EMT is compared against the small signal model with and without modelling the angle ' $\phi$ '. The responses are shown in Fig. 9.

When ' $\phi$ ' is ignored, oscillatory behaviour is observed as expected. The importance of modelling the phase shift further supports the argument that the inherent damping is represented in the dynamic phasor model through the phase shift between opposite polarity peaks of the line current and TCR current, which adds damping to the circuit.

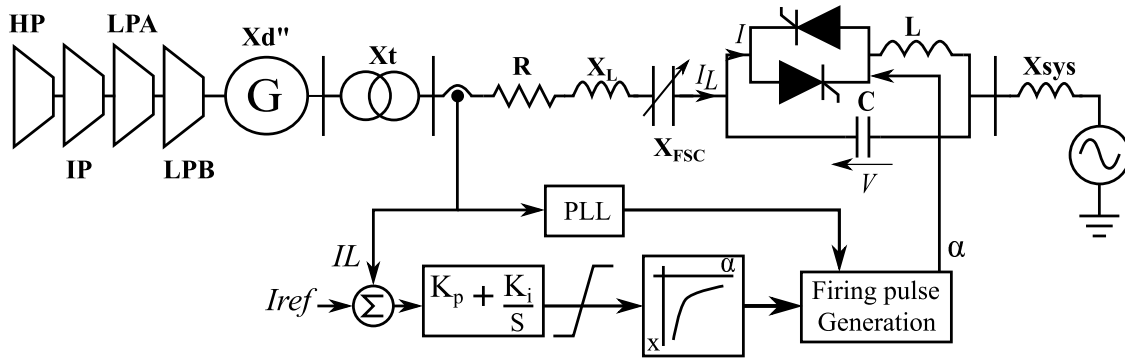


FIGURE 10. IEEE 1<sup>st</sup> Benchmark model for SSR studies modified to include a TCSC.

### VI. EVALUATION OF INHERENT DAMPING OF TCSC

IEEE 1<sup>st</sup> benchmark model for SSR studies [34] is used to demonstrate the effect of inherent damping capability of the TCSC on IGE and TI. The effect of adding the TCSC is evaluated under two cases, A) IGE and B) TI, in contrast to having an FSC. The series compensation is achieved with either an FSC or a TCSC or a combination of both, as shown in Fig. 10. TCSC is operated in open loop configuration with a fixed firing angle to demonstrate its inherent damping nature (i.e. no supplementary controls are used). However, the effect of operating the TCSC in closed loop current control mode is also evaluated at the end. A nominal series compensation level of 45% and 31% is assumed for each case study (IGE and TI). The level of compensation is then varied by either changing the size of the FSC or changing the firing angle of an equivalent TCSC. In both cases A and B, the TCSC is designed according to (1), (2), and (3), such that it provides the nominal series compensation level at a boost factor of 1.3 with a characteristic factor of 2.5.

#### A. EFFECT OF TCSC ON INDUCTION GENERATOR EFFECT

IGE is clearly observable when there is no electrical damping from the network elements. Thus, the resistance ‘R’ in Fig. 10 is assumed to be zero for this case. Furthermore, the exciter dynamics are ignored and the multi-mass model is disabled to avoid any interactions with torsion modules. The series compensation is varied from 34.5% to 110 % first with an FSC and then with a TCSC by changing its firing angle (which effectively changes its boost factor). The minimum compensation level of 34.5% is achieved when the firing angle of the TCSC is at 90<sup>0</sup> (blocked thyristor mode), i.e. the boost factor is 1 and the TCSC behaves as an FSC. A compensation level as high as 110% was considered to analyze the full range of operation of the TCSC in the capacitive vernier mode. Small signal stability of the system is evaluated at each compensation level in both scenarios. Frequency and damping of the network mode versus the compensation level is shown in Fig. 11. Network mode frequencies are expressed in rotor reference frame (complement to 60Hz). The network mode is negatively damped at all times with an FSC in the

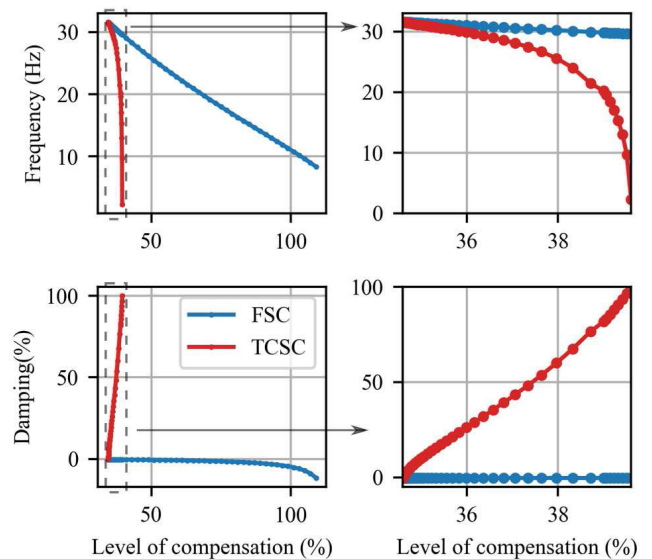
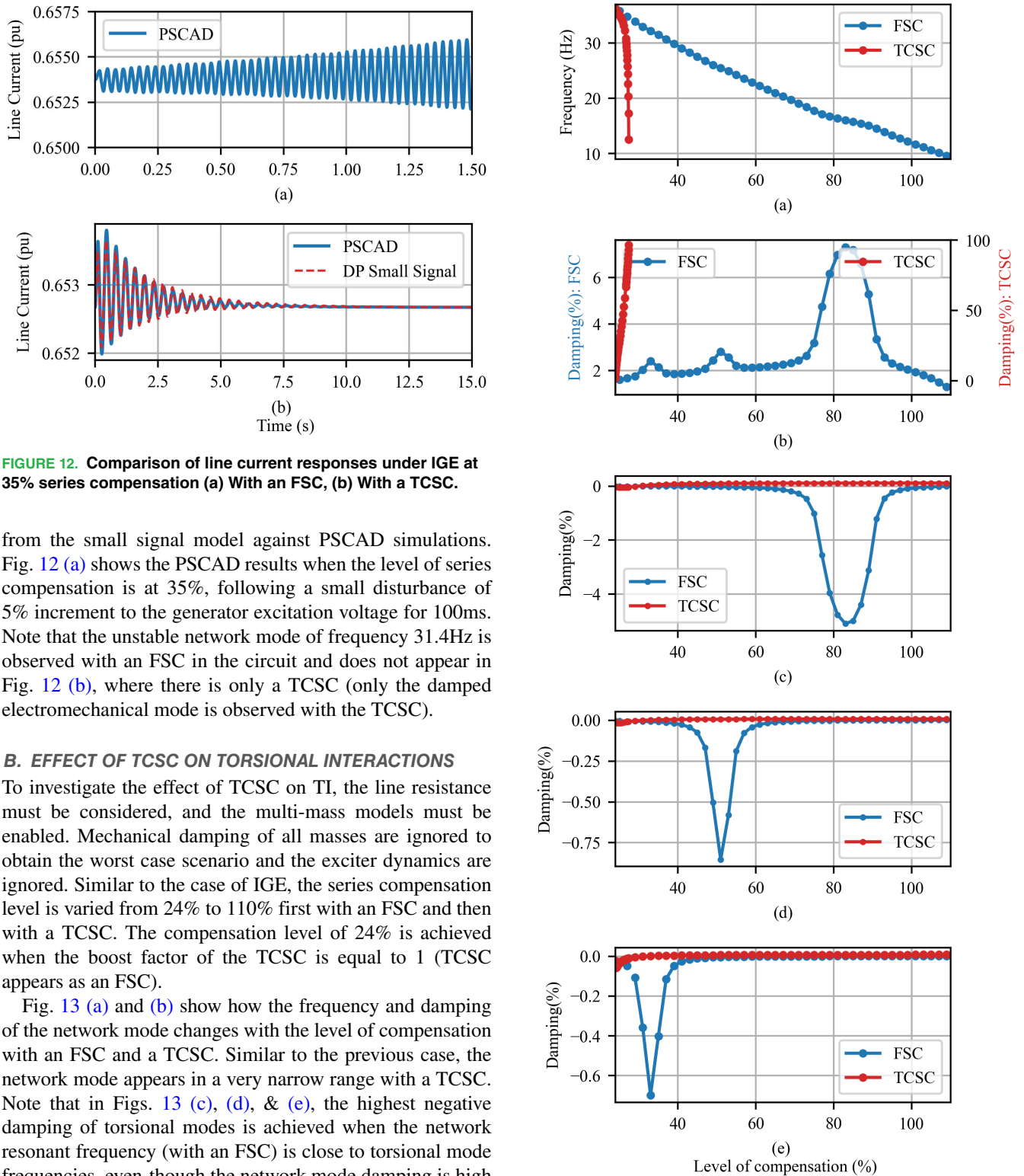


FIGURE 11. Frequency (with respect to rotor reference frame) and damping of the network mode Vs. level of compensation: IGE. (Plots to the right are the zoomed regions in which the network mode exist when a TCSC is used).

network, and the damping further reduces with increasing levels of series compensation. This is purely due to the negative resistance from the synchronous generator rotor to sub-synchronous currents.

Using a TCSC instead of an FSC showed a good improvement in the network mode damping. When the TCSC boost factor is 1 (Firing angle = 90<sup>0</sup>), the behaviour is very close to that of the FSC. As the boost factor is increased, the compensation level increases and the network mode appears in a very narrow range of compensation level from 34.6% to 39.6%, beyond which it disappears due to the inductive nature of the TCSC at sub-synchronous frequencies. Within the range of 34.6% to 39.6%, it is seen that the network resonant frequency changes drastically compared to that of an FSC. More importantly, the network mode is well damped compared to that of the FSC and the damping improves rapidly to 100%. Thus, it can be claimed that the inductive & resistive nature of the TCSC at sub-synchronous frequencies eliminates the IGE. Fig. 12 shows the comparison of line current responses



**FIGURE 12.** Comparison of line current responses under IGE at 35% series compensation (a) With an FSC, (b) With a TCSC.

from the small signal model against PSCAD simulations. Fig. 12 (a) shows the PSCAD results when the level of series compensation is at 35%, following a small disturbance of 5% increment to the generator excitation voltage for 100ms. Note that the unstable network mode of frequency 31.4Hz is observed with an FSC in the circuit and does not appear in Fig. 12 (b), where there is only a TCSC (only the damped electromechanical mode is observed with the TCSC).

**B. EFFECT OF TCSC ON TORSIONAL INTERACTIONS**

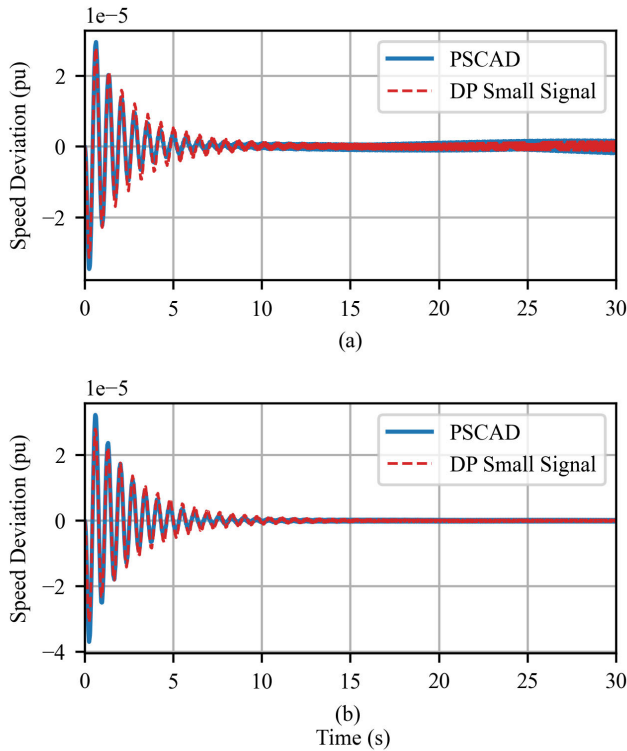
To investigate the effect of TCSC on TI, the line resistance must be considered, and the multi-mass models must be enabled. Mechanical damping of all masses are ignored to obtain the worst case scenario and the exciter dynamics are ignored. Similar to the case of IGE, the series compensation level is varied from 24% to 110% first with an FSC and then with a TCSC. The compensation level of 24% is achieved when the boost factor of the TCSC is equal to 1 (TCSC appears as an FSC).

Fig. 13 (a) and (b) show how the frequency and damping of the network mode changes with the level of compensation with an FSC and a TCSC. Similar to the previous case, the network mode appears in a very narrow range with a TCSC. Note that in Figs. 13 (c), (d), & (e), the highest negative damping of torsional modes is achieved when the network resonant frequency (with an FSC) is close to torsional mode frequencies, even-though the network mode damping is high at these points. When the same compensation levels are achieved with a TCSC, all three torsional modes are damped above the level of 31% compensation, eliminating the risk of torsional interactions. Fourth torsional mode (TM4 frequency: 47.45 Hz) is neither observable nor controllable at the generator and therefore is not included in the figures. To further validate the observations from the small signal analysis,

**FIGURE 13.** Effect of TCSC on torsional modes compared with an FSC. (a) Network mode frequency (b) Network mode damping (c) TM1: 16.25 Hz, (d) TM2: 25.43 Hz, (e) TM3: 32.19 Hz.

time domain responses of generator speed deviations at 25% and 31% compensation are illustrated in Fig. 14 (a) and (b) respectively.





**FIGURE 14.** Comparison of generator speed deviation at (a)25% series compensation (Unstable), (b) 31% series compensation (Stable).

It should be further noted that, the narrow range of network resonant frequencies with significantly high damping is observable with a TCSC regardless of the selected nominal compensation level. The network mode appears only when the firing angle is close to  $90^0$ .

A TCSC can be designed to operate at the nominal series compensation level, based on the choice of two parameters, a) Boost factor and b) The level of controllable series compensation. In the previous two cases, the TCSC was designed to provide the total nominal series compensation level at a boost factor of 1.3 and with a characteristic factor of 2.5. It is worth to investigate how the choice of aforementioned parameters effect the torsional modes when operating at the nominal series compensation level. When the nominal series compensation level of 31% is fully achieved with a TCSC, the sensitivity of torsional mode damping to the boost factor is shown in Fig. 15. Inductance ‘L’ and capacitance ‘C’ of the TCSC are chosen according to (1), (2), and (3) at each boost factor with a constant characteristic factor ( $\lambda$ ) of 2.5. Better damping of torsional modes is achieved at high boost factors. Then, choosing a nominal boost factor of 1.3, the TCSC level is changed from 10% to 100% while maintaining the total series compensation at the nominal value of 31% with an FSC. Note that the ‘L’ and ‘C’ of the TCSC are chosen same as before at every compensation level with a constant characteristic factor ( $\lambda$ ) of 2.5. It is clear from Fig. 16 that high TCSC levels improve the damping of torsional modes.

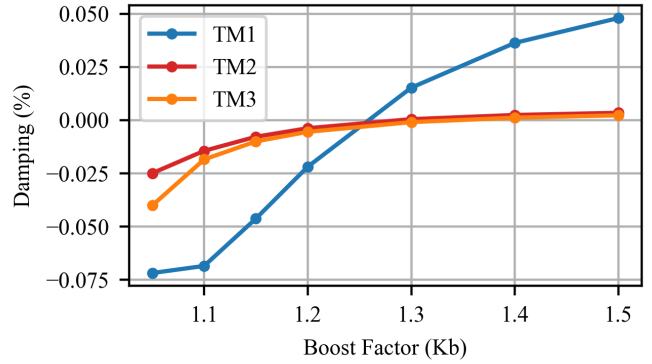


**FIGURE 15.** Effect of Boost factor on Torsional Mode(TM) damping. Series compensation at 31%. TM1: 16.25 Hz, TM2: 25.43 Hz, & TM3: 32.19 Hz.

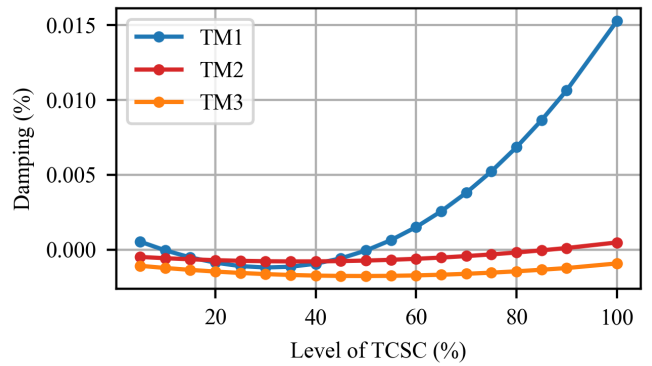


**FIGURE 16.** Effect of TCSC level on torsional modes. Boost factor =1.3. TM1: 16.25 Hz, TM2: 25.43 Hz, & TM3: 32.19 Hz.

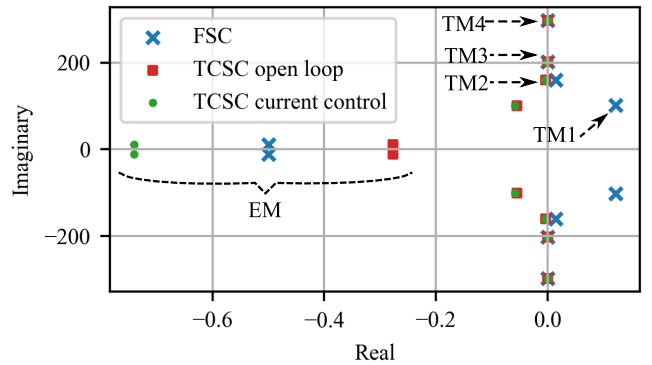


**FIGURE 17.** Effect of adding current controller on torsional modes and Electro-Mechanical (EM) mode.

Up to now, the TCSC was mainly analysed in constant firing angle mode. But practical projects also adopts closed loop controls such as voltage control, power flow control and current control [16], [17]. The effect of adding a basic current controller (controller parameters:  $K_p = 5$ ,  $K_i = 150$ ) is illustrated in Fig. 17. The closed loop current control of TCSC has no impact on torsional modes and this behavior is expected as the controller is not designed to eliminate SSR risks. As for the electro-Mechanical (EM) mode, damping has decreased when the TCSC is introduced and operated with

fixed firing angle, but when it is operated with current control mode, damping improves compared to the FSC scenario.

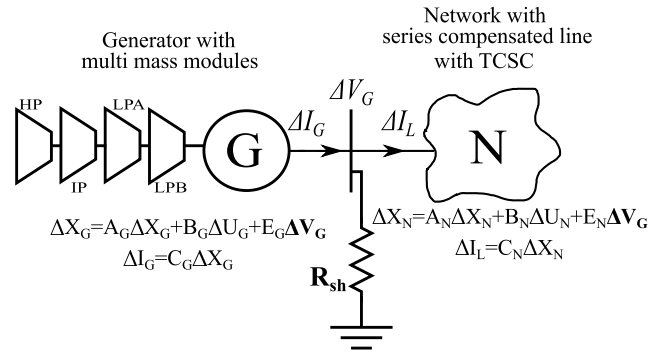
## VII. CONCLUSION

The inherent damping capability of the TCSC at sub-synchronous frequencies is analysed in this paper through small signal stability analysis of a simplified DP model of the TCSC. It is shown that the non-linearity in thyristor switching behaviour (which is modelled as a phase shift between the opposite polarity peaks of the line current and thyristor current in the DP model) appears as a dynamic resistance and contributes to the inherent damping nature of the TCSC. Small signal stability analysis of the IEEE 1<sup>st</sup> benchmark model with a TCSC showed that, the network mode exists only when the TCSC is operated very close to a boost factor of '1'. The network mode appears in a very narrow range of compensation levels and the damping of the network mode is much higher than that of the FSC in this region. The risk of IGE and TI is avoided due to the absence of a network mode and resistive nature of the TCSC at sub-synchronous frequencies. However, if the TCSC is operated below its nominal operating point it is designed to (low boost factors), there may still be a risk of TI. Such operating conditions may need SSDC.

Based on similar evaluations, one can design the TCSC to achieve a minimum TCSC level, with a proper boost factor to avoid existing SSR problems at the design stage or simply increase the operational boost factor to obtain more damping to SSR conditions. Time domain responses of the IEEE 1<sup>st</sup> benchmark model with TCSC is in good agreement with the simplified DP small signal model and therefore the model is recommended for SSR analysis. The proposed method can be used to evaluate whether the inherent damping of TCSC is sufficient to avoid SSR conditions at the planning stage, given a safety margin. If not, additional subsynchronous damping controllers can be attached to the TCSC and the design of the controller can be carried out using the small signal stability model proposed in this paper. The simplified DP model is fundamental frequency based and is readily compatible with phasor based models of other power system components and can easily be implemented in commercial small signal assessment tools.

## APPENDIX INTERFACING GENERATOR AND NETWORK WITH TCSC

Figure below shows how small signal models of the generator and the network in Fig. 10 are interfaced. Current injection from the generator ( $\Delta I_G$ ) and the network ( $\Delta I_L$ ) can be expressed in terms of generator and network state variables respectively. Similar to EMT type programs, a large fictitious resistor ' $R_{sh}$ ' is connected at the interface bus to avoid any numerical instabilities which can occur when interfacing two independent state variables [35]. However, if there is a resultant shunt capacitance at the terminal (e.g. tx line), there is no need for a fictitious resistor.



The network model is obtained as in Fig. 5 which is a combination of transmission line, system and generator transformer impedance and TCSC. The interface bus voltage ' $V_G$ ' is then calculated as in (16) and substituted in generator and network state equations to obtain the combined state space model of the system.

$$\Delta V_G = R_{sh}(\Delta I_G - \Delta I_L) \quad (16)$$

## REFERENCES

- [1] P. Kundur, N. J. Balu, and M. G. Lauby, "Sub-synchronous resonance," in *Power System Stability and Control*, vol. 7. New York, NY, USA: McGraw-Hill, 1994, pp. 1025–1105.
- [2] J. Adams, C. Carter, and S.-H. Huang, "ERCOT experience with sub-synchronous control interaction and proposed remediation," in *Proc. IEEE PES Transmiss. Distrib. Conf. Expo*, May 2012, pp. 1–5.
- [3] "Proposed terms and definitions for subsynchronous oscillations," *IEEE Trans. Power App. Syst.*, vol. PAS-99, no. 2, pp. 506–511, Mar. 1980.
- [4] P. M. Anderson, B. L. Agrawal, and J. E. Van Ness, *Subsynchronous Resonance in Power Systems*. New York, NY, USA: IEEE Press, 1990.
- [5] D. N. Walker, C. E. J. Bowler, R. L. Jackson, and D. A. Hodges, "Results of subsynchronous resonance test at Mohave," *IEEE Trans. Power App. Syst.*, vol. PAS-94, no. 5, pp. 1878–1889, Sep. 1975.
- [6] L. Wang, X. Xie, Q. Jiang, H. Liu, Y. Li, and H. Liu, "Investigation of SSR in practical DFIG-based wind farms connected to a series-compensated power system," *IEEE Trans. Power Syst.*, vol. 30, no. 5, pp. 2772–2779, Sep. 2015.
- [7] X. Xie, X. Zhang, H. Liu, H. Liu, Y. Li, and C. Zhang, "Characteristic analysis of subsynchronous resonance in practical wind farms connected to series-compensated transmissions," *IEEE Trans. Energy Convers.*, vol. 32, no. 3, pp. 1117–1126, Sep. 2017.
- [8] R. M. Mathur and R. K. Varma, "Applications of TCSC," *Thyristor-Based Facts Controllers for Electrical Transmission Systems*. Piscataway, NJ, USA: IEEE Press, 2002.
- [9] X. Zheng, Z. Xu, and J. Zhang, "A supplementary damping controller of TCSC for mitigating SSR," in *Proc. IEEE Power Energy Soc. Gen. Meeting*, Jul. 2009, pp. 1–5.
- [10] M.-Q. Tran et al., "Analysis and mitigation of subsynchronous resonance in a Korean power network with the first TCSC installation," *Energies*, vol. 12, pp. 1–16, Jul. 2019.
- [11] D. Holmberg, M. Danielsson, P. Halvarsson, and L. Angquist, "The stode thyristor controlled series capacitor," in *Proc. CIGRE Paris Gen. Session*, Paris, France, 1998. [Online]. Available: [https://e-cigre.org/publication/14-105\\_1998-the-stode-thyristor-controlled-series-capacitor](https://e-cigre.org/publication/14-105_1998-the-stode-thyristor-controlled-series-capacitor)
- [12] K. Dey, M. K. Das, and A. M. Kulkarni, "Comparison of dynamic phasor, discrete-time and frequency scanning based SSR models of a TCSC," *Electr. Power Syst. Res.*, vol. 196, Jul. 2021, Art. no. 107237.
- [13] S. R. Joshi, E. P. Cheriyan, and A. Kulkarni, "Output feedback SSR damping controller design based on modular discrete-time dynamic model of TCSC," *IET Gener. Transmiss. Distrib.*, vol. 3, no. 6, pp. 561–573, Jun. 2009.

- [14] L. Angquist, "Synchronous voltage reversal control of thyristor controlled series capacitor," Ph.D. dissertation, Dept. Elect. Eng., Royal Inst. Technol., Stockholm, Sweden, 2002.
- [15] W. Zhu, R. Spee, R. R. Mohler, G. C. Alexander, W. A. Mittelstadt, and D. Maratukulam, "An EMTP study of SSR mitigation using the thyristor controlled series capacitor," *IEEE Trans. Power Del.*, vol. 10, no. 3, pp. 1479–1485, Jul. 1995.
- [16] L. A. S. Pilotto, A. Biamco, W. F. Long, and A. Edris, "Impact of TCSC control methodologies on subsynchronous oscillations," *IEEE Trans. Power Del.*, vol. 18, no. 1, pp. 243–252, Jan. 2003.
- [17] N. Chistl et al., "Advanced series compensation (ASC) with thyristor controlled impedance," in *Proc. CIGRE Paris General Session*, Paris, France, 1992. [Online]. Available: [https://e-cigre.org/publication/14-37-38\\_05\\_1992-advanced-series-compensation-asc-with-thyristor-controlled-impedance](https://e-cigre.org/publication/14-37-38_05_1992-advanced-series-compensation-asc-with-thyristor-controlled-impedance)
- [18] S. Nyati, C. A. Wegner, R. W. Delmerico, R. J. Piwko, D. H. Baker, and A. Edris, "Effectiveness of thyristor controlled series capacitor in enhancing power system dynamics: An analog simulator study," *IEEE Trans. Power Del.*, vol. 9, no. 2, pp. 1018–1027, Apr. 1994.
- [19] A. Daneshpoooy and A. M. Gole, "Frequency response of the thyristor controlled series capacitor," *IEEE Trans. Power Del.*, vol. 16, no. 1, pp. 53–58, Jan. 2001.
- [20] K. Kabiri, S. Henschel, and H. W. Dommel, "Resistive behavior of thyristor-controlled series capacitors at subsynchronous frequencies," *IEEE Trans. Power Del.*, vol. 19, no. 1, pp. 374–379, Jan. 2004.
- [21] R. Zheng, "SSR mitigation with TCSC in power systems," Ph.D. dissertation, School Eng., Univ., Cardiff, Cardiff, U.K., 2017.
- [22] G. Jalali, R. H. Lasseter, and I. Dobson, "Dynamic response of a thyristor controlled switched capacitor," *IEEE Trans. Power Syst.*, vol. 9, no. 3, pp. 1609–1615, Jul. 1994.
- [23] A. Ghosh and G. Ledwich, "Modelling and control of thyristor-controlled series compensators," *IEE Proc. Gener. Transmiss. Distrib.*, vol. 142, no. 3, pp. 297–304, May 1995.
- [24] R. Rajaraman, I. Dobson, R. H. Lasseter, and Y. Shern, "Computing the damping of subsynchronous oscillation due to a thyristor controlled series capacitor," *IEEE Trans. Power Syst.*, vol. 11, no. 2, pp. 1120–1127, Apr. 1996.
- [25] H. A. Othman and L. Angquist, "Analytical modeling of thyristor-controlled series capacitors for SSR studies," *IEEE Trans. Power Syst.*, vol. 11, no. 1, pp. 119–127, Feb. 1996.
- [26] B. K. Perkins and M. R. Iravani, "Dynamic modeling of a TCSC with application to SSR analysis," *IEEE Trans. Power Syst.*, vol. 12, no. 4, pp. 1619–1625, Nov. 1997.
- [27] K. Kabiri, S. Henschel, J. R. Marti, and H. W. Dommel, "A discrete state-space model for SSR stabilizing controller design for TCSC compensated systems," *IEEE Trans. Power Del.*, vol. 20, no. 1, pp. 466–474, Jan. 2005.
- [28] S. R. Joshi and A. M. Kulkarni, "Comparative evaluation of discrete-time dynamic models of TCSC," in *Proc. 16th Power Syst. Comput. Conf.*, Jul. 2008, pp. 14–18.
- [29] P. Mattavelli, G. C. Verghese, and A. M. Stankovic, "Phasor dynamics of thyristor-controlled series capacitor systems," *IEEE Trans. Power Syst.*, vol. 12, no. 3, pp. 1259–1267, Aug. 1997.
- [30] P. Mattavelli, A. M. Stankovic, and G. C. Verghese, "SSR analysis with dynamic phasor model of thyristor-controlled series capacitor," *IEEE Trans. Power Syst.*, vol. 14, no. 1, pp. 200–208, Feb. 1999.
- [31] T. Demiray, "Simulation of power system dynamics using dynamic phasor models," Ph.D. dissertation, Swiss Federal Inst. Tech, Zurich, Germany, 2008.
- [32] R. Zheng, G. Li, and J. Liang, "Capability of TCSC on SSR mitigation," *J. Power Energy Eng.*, vol. 3, no. 4, pp. 232–239, 2015.
- [33] C. Karawita, "HVDC interaction studies using small signal stability assessment," Ph.D. dissertation, Dept. Elect., Comp. Eng., Univ. Manitoba, Manitoba, 2009.
- [34] IEEE SSR Working Group, "First benchmark model for computer simulation of subsynchronous resonance," *IEEE Trans.*, vol. PAS-96, no. 5, pp. 1565–1572, Sep/Oct. 1977.

- [35] D. H. R. Suriyaarachchi, "Sub-synchronous interactions in a wind integrated power system," Ph.D. dissertation, Dept. Elect., Comp. Eng., Univ. Manitoba, Manitoba, 2014.



**D. R. WEERAKOON** (Graduate Student Member, IEEE) received the B.Sc. (Eng.) degree from the Sri Lanka Institute of Information Technology, Malabe, Sri Lanka, in 2017. She is currently pursuing the Ph.D. degree with the University of Manitoba, Winnipeg, MB, Canada.

She is also a contributor to the CIGRE Working Group C4/B4.52 "Guidelines for Sub-synchronous Oscillation Studies in Power Electronics Dominated Power Systems." Her

research interests include sub-synchronous resonance in power systems and dynamic phasor modeling of FACTS devices.



**C. KARAWITA** (Senior Member, IEEE) received the B.Sc. (Eng.) degree from the University of Moratuwa, Moratuwa, Sri Lanka, in 2002, and the M.Sc. and Ph.D. degrees from the University of Manitoba, Winnipeg, MB, Canada, in 2006 and 2009, respectively.

In 2007, he joined TransGrid Solutions Inc., Canada, where he is working as the Vice President-Studies. He is currently the Convener of Working Group C4/B4.52 "Guidelines for

Sub-synchronous Oscillation Studies in Power Electronics Dominated Power Systems" and involved in academic research activities as an Adjunct Professor at the University of Manitoba. He is also an expert in power system studies, including HVAC, HVDC and FACTS, and inverter based on generation (Solar, Wind, and BESS). He was instrumental in developing a software package (TGSSR) to analyze subsynchronous interactions.



**U. D. ANNAKAGE** (Senior Member, IEEE) received the B.Sc. (Eng.) degree from the University of Moratuwa, Sri Lanka, in 1982, and the M.Sc. and Ph.D. degrees from the University of Manchester Institute of Science and Technology (UMIST), Manchester, U.K., in 1984 and 1987, respectively.

He is currently a Professor with the Department of Electrical and Computer Engineering, University of Manitoba, Canada. He has more than

35 years of experience in teaching, research, and consulting. His main strength is in power system stability and security assessment.